Laser Ablation-Capillary Absorption Spectroscopy: A novel approach for high throughput and increased spatial resolution measurements of $\delta^{13}C$ in plant-soil systems

Daniel M. Cleary[1,2,3], Timothy J. Linley[4], Jason M. Kriesel[5], Andrew Fahrland[5], James F. Kelly[5], James J. Moran[1,6*]

[1] Pacific Northwest National Laboratory, Environmental Molecular Sciences Laboratory, Richland, WA, U.S.A.

[2] Center for Climate Physics, Institute for Basic Science, Busan, Republic of Korea, 46241

[3] Department of Atmospheric Sciences, Pusan National University, Busan, Republic of Korea, 46241

[4] Pacific Northwest National Laboratory, Earth and Environment Directorate, Richland, WA, U.S.A.

[5] Opto-Knowledge Systems, Inc., Torrance, CA, U.S.A.

[6] Current: Michigan State University, Departments of Integrative Biology and Plant, Soil, and Microbial Sciences, East Lansing, MI, U.S.A.

*Correspondence: moranja7@msu.edu

Abstract:

Spatial and temporal heterogeneity of nutrient exchange within the rhizosphere is a topic of increasing interest, although challenging to study due to limits in existing analytical capabilities. Here, we developed and demonstrated a new approach applying laser ablation sample introduction to capillary absorption spectroscopy (LA-CAS) to characterize carbon isotopic distribution within plant tissues, rhizosphere, and soil. We exposed switchgrass plants to $^{13}CO_2$ to allow tracing of ^{13}C-labelled photosynthates within plant biomass and into the associated soil. The LA-CAS methods we describe leverage continuous measurements of a sample stream derived from laser ablation line scans (10-25 μm in width) over a sample surface which enables the user to produce an isotope map with a) higher data density or b) over larger spatial areas versus previously existing techniques. This versatility of LA-CAS is assessed through testing of a range of laser parameters (spot size, scan rates) on various materials (soil, plant biomass/tissues, and rhizosphere). We demonstrate the ability of LA-CAS to provide near instantaneous $\delta^{13}C$ measurements over isotopically distinct surfaces to enable high spatially resolved mapping of ^{13}C-labelled material within the rhizosphere. Applying LA-CAS analysis to plant biomass, we observed higher $\delta^{13}C$ values concentrated within phloem structures, consistent with localized photosynthate transport. When mapping across the rhizosphere, ^{13}C-enriched soil was typically present within a 5-10 μm of root boundaries with a steep spatial increase in $\delta^{13}C$

when the scan approached the middle of the root. As with all LA approaches, care needs to be taken to ensure accurate results as phenomena linked to matrix-dependent shifts in ablation behavior/efficiency, variability created by surface topography in the sample, and dependence on complete combustion of the ablated particulates can all impact ultimate usefulness of the data. Still, taken as a whole, our demonstrations highlight the increased sample throughput and resulting data density of using LA-CAS versus other LA techniques (i.e., when coupled to isotope ratio mass spectrometry) for performing spatially specific $\delta^{13}C$ measurements within plant and rhizosphere systems, the resulting improvements in mapping of carbon introduced into these dynamic systems, and emphasize the role this method can play in future plant and rhizosphere related studies.

Keywords: stable isotope analysis, rhizosphere, root exudate, switchgrass, isotope mapping

1. Introduction

Measurement and analysis of stable isotopes offers a reliable approach for characterizing biogeochemical processes at the soil and plant levels (Bird et al. 2011; Holz et al. 2018). Such studies have the potential to better define the biogeochemical fluxes between plant roots and soil systems. Of particular interest is the flux of plant-derived organic carbon provided to soil through the rhizosphere (Lambers et al. 2009). Soil microbial communities are reliant on this source of carbon and can, in turn, improve microbially mediated nutrient exchange with plants (Bais et al. 2006; Hinsinger et al. 2005). However, the location where carbon-containing exudates are concentrated within the rhizosphere and surrounding soil is often spatially and temporally variable. For example, plants will preferentially direct root growth towards nutrient rich soil, creating a localized increase in biogeochemical activity (Hodge 2004; Kuzyakov and Blagodatskaya 2015). This spatial heterogeneity can be further accentuated as the result of root differentiation and the lifespan of specialized sections of a root system (Hinsinger et al. 2009; Hinsinger et al. 2005; Marschner et al. 2011). Understanding the complexities of this system is crucial for optimizing conditions for biomass productivity, avoiding nutrient depletion, and reducing the agricultural dependency on synthetic fertilizers (de Vrieze 2015; Hinsinger et al. 2009). While there is substantial interest in rhizosphere related research, the small spatial dimension (processes and gradients at the µm – to mm ranges) of rhizosphere presents challenges for conventional analytical techniques (Moran and McGrath 2021).

Rhizodeposition represents one of the primary modes of delivering photosynthates to the soil (Pausch and Kuzyakov 2018). A practical approach to defining spatial heterogeneity of rhizodeposition is through carbon isotope ($\delta^{13}C$) analysis using a $^{13}CO_2$ tracer (Kuzyakov and Domanski 2000). When coupled to a suitable analysis technique, the resulting plant derived ^{13}C-labeled nutrients can be tracked into and their distribution mapped through the rhizosphere (Denis et al. 2019). However, these efforts can be constrained by the spatial resolution and time required for analysis associated with the instrumentation. Laser ablation-isotope ratio mass spectrometry (LA-IRMS) is a technique able to provide precise $\delta^{13}C$ measurements and allow mapping at sub-mm scales (Bruneau et al. 2002). Due to limited sensitivity of IRMS (Li et al. 2018; nmol to μmol C required per measurement), however, the minimum spot size for ablation is roughly 10-25 μm and the needed cryofocusing of sample-derived CO_2 is a time consuming / low throughput step that can limit the number of spatially resolved data points (Denis et al. 2019; Grieve et al. 2006; Rodionov et al. 2019). Other methods such as nanoscale secondary ion mass spectrometry (NanoSIMS) can allow for isotope imaging at ~100 nm scale (Clode et al. 2009) but require extensive time for sample preparation and analysis, are restricted to relatively small sample areas of analysis, and are a comparatively expensive analytical platform with restricted availability for many investigations.

Although new relative to other methods, capillary absorption spectroscopy (CAS) is an effective technique for analysis of carbon stable isotopes (Kelly et al. 2012). Considering the lower sample size requirements for isotope measurements (as little as 1 picomole of CO_2; Kelly et al. 2012), CAS may be a suitable alternative for isotope mapping at more sensitive spot sizes (versus LA-IRMS) over mm length scales (Kriesel et al. 2020). The sensitivity of CAS results from the interaction between light generated by a continuous wave tunable laser and analyte within a low volume hollow waveguide fiber maintained at low pressure. Additionally, isotopic analysis within a CAS system is inherently non-destructive which can allow for recirculation of an analyte gas back into an experimental system to enable, for example, measurements such as continuous tracking of respired CO_2 in soil systems (Cleary et al. 2021). A similar setup, but without sample recirculation, could enable continuous flow $\delta^{13}C$ measurements of CO_2 in an analyte stream. Recent work demonstrated the feasibility of coupling LA to CAS, however, this was performed using batch isotope analysis by CAS whereby each sample was cryogenically trapped then introduced into the CAS system for analysis; a time consuming step which limits sample throughput and the data density in the resulting maps of sample $\delta^{13}C$ (Moran et al. 2022).

In this study, we assess and demonstrate the potential for combining the sensitivity and flow-through nature of CAS with laser ablation sampling to enable continuous flow measurements of $\delta^{13}C$ for the purposes of performing high spatial resolution mapping of rhizosphere and plant tissue samples. We chose a specific soil and plant type to test LA-CAS because 1) this pairing has been previously demonstrated to produce partial, spatially differentiated ^{13}C enrichment in plant tissue and rhizosphere samples used in LA-IRMS (Denis et al. 2019) and LA-CAS (Moran et al. 2022) studies, 2) the soil and plant are well characterized, originate from a long term ecological research station, and have been used in a wide range of previous studies, and 3) methods demonstrated on this plant and soil pair should be broadly applicable to a wide range of other varieties. While we will effectively consider the suitability of this material, the methodology should be applicable when considering ^{13}C distribution in other solid-state materials. We employ a continuous line scan and quantify the flow rates from ablation to measurement to determine any potential mixing of sample derived from different laser ablation pulses (which would limit spatial resolution). As additional verification, $\delta^{13}C$ was compared between 25 μm spot size ablations made in proximity to a line scan. Subsequently, a series of single continuous line scans were made over isotopically distinct materials. Each of these experiments allowed for the determination of how accurately and efficiently CAS can capture gradual and abrupt spatial changes in a sample's $\delta^{13}C$. To ensure the resulting $\delta^{13}C$ profile for a scan is reproducible, a segmented line ablation was performed with the beam turning and continuing in the reverse direction parallel to the initial path. The utility of this continuous measurement was then leveraged to produce a high spatial resolution $\delta^{13}C$ map of the internal structure of a ^{13}C-labelled root. Lastly, we expanded this approach to carbon isotope mapping of a ^{13}C-tracer within a rhizosphere-soil sample over a 2-3 mm sampling window to demonstrate the ability to map relatively large surfaces of a sample.

2. Materials and methods

2.1 LA-CAS system

For sample introduction, the CAS instrument was interfaced with a CETAC LSX-500 (Teledyne CETAC, Omaha, NE) laser ablation system (266 nm Nd:YAG laser; **Fig. 1**). Ablated particulates were entrained in a helium carrier gas and passed through ~30 cm of stainless steel tubing (1 mm ID) from the LSX-500 (**Fig.1A**) to a micro-combustion reactor (**Fig.1B**) for conversion to CO_2. This sample-derived CO_2 subsequently traveled through a second section of stainless steel tubing (22 cm), a 20 cm length (0.52 mm ID) fused silica capillary (used for strain relief), and then entered the CAS system.

As it passed into and through the CAS fiber, the sample-derived CO_2 was analyzed using a tunable distributed feedback interband cascade laser with an output wavelength centered at 4355.4 (2296 cm^{-1}) and measured absorbance by the analyte using a mercury cadmium telluride (MCT) detector (PVI-5-1x1-TO39-NW-36 by Vigo Photonics, Ożarów Mazowiecki, Poland). This targeted wavelength region is in the mid-infrared range and has separate absorption features for $^{13}C^{16}O_2$ and $^{12}C^{16}O_2$ that are measured for determination of $\delta^{13}C$ as described in (Cleary et al. 2021). After a sample is measured for $\delta^{13}C$ using CAS, the CO_2 is removed from the fiber and evacuated to lab atmosphere via pumping with a small diaphragm vacuum (**Fig. 1D**).

2.2 Calibrating travel time of analyte

A 10 µm spot size line ablation pass was completed on a piece of commercially purchased Lexan material ($\delta^{13}C$ = -14.2 ± 3.5 ‰) at 5 µm sec^{-1} horizontal scanning speed. Our previous work with this and similar materials suggested the Lexan would have consistent isotopic content within the acquired sheet and could thus serve as a reference material for comparing between different sample analyses. Data acquisition proceeded at one measurement every 0.82 seconds over the ~500 µm path (**Fig. 2**). The time (T) since first contact of the laser beam with surface (T_1) was monitored manually and logged for events; T_2) first appearance of analyte reaching the CAS, T_3) stabilization around the mean raw $\delta^{13}C$ of the material, T_4) end of ablation, T_5) last measurement of sample and T_6) return to pre ablation baseline. Seven analytical replicates of this analysis were completed.

2.3 Determining CAS response when ablating over isotopically distinct surfaces

To consider the applicability of this approach, a sectioned switchgrass (*Panicum virgatum* variety Cave-in-rock) stem was placed within a trench cut in the middle of a Lexan cube (same material as used in 2.2). During growth, the switchgrass was exposed to a $^{13}CO_2$ label for two diurnal photosynthetic cycles. We observed elevated $\delta^{13}C$ values of rhizosphere samples indicated release of photosynthetically derived organic material suggestive of labeling plant biomass and metabolites. A continuous 25 µm spot size line ablation was completed on the stem (bracketed by Lexan on both sides) at a linear rate of 5 µm sec^{-1}. The analysis occurred over 4.5 mm with data acquisition at one measurement every 0.82 seconds. The scan was repeated in the reverse direction on a nearby location of the same stem to gauge repeatability of spatial shifts in measured $\delta^{13}C$ (results presented in Section 3.2 and **Fig. 3**).

Using a second example, the same procedure and laser parameters were applied to a puck with ^{13}C labeled soil and root in addition to a section of fishing line used for calibration. The fishing line used (Premium Plus 7 monofilament,15# test nylon line; Danielson, Auburn, WA, USA) was previously described and calibrated ($\delta^{13}C$ = -27.7‰; Moran et al., 2011) and used here as an isotope standard for data calibration. During the experiment, ablation progressed from 1) soil, to 2) fishing line, to 3) soil, to 4) root and to 5) soil. Ten spot ablations were performed in proximity to the continuous line ablation transect. For each spot ablation, analyte was trapped internally within the CAS and analyzed for 90 seconds (110 measurements). Trapping was achieved by automated valve closure at both inlet and outlet ends of the CAS, allowing recirculation of analyte. Initialization of trapping was set to begin once a desired concentration was reached in the detector. The resulting spot assessment of $\delta^{13}C$ was compared to the corresponding coeval isotopic data recorded along the continuous line transect (**Fig. 4**). We also performed a series of scans alternating between different spot sizes and scan rates capturing soil, rhizosphere, and roots. We completed multiple scans over the same root with a 25 µm spot size and 10 µm sec^{-1} rate for soil and 10 µm/5 µm sec^{-1} for root to assess if a set of parameters was more ideal for each material (**Fig. 5**).

2.4 Continuous flow ablation in two directions

We demonstrated the ability of the continuous flow LA-CAS method to be applied to larger spatial areas by performing a continuous line ablation along a transect including ^{13}C labeled soil and root and a piece of fishing line for calibration. We performed a transect in two directions to test the reproducibility of data stream and assess any potential memory effects that may occur as the beam passes through isotopically distinct surfaces. The samples ablated in the first pass occurred in the order described in 2.3. We continued the beam/ablation path and subsequently produced an ablation transect parallel to the first (using a reverse order of material being sampled). A 25 µm spot size was used during line ablation moving at a rate of 5 µm sec^{-1}. The resulting data are presented in section 3.3 and **Fig. 6**.

2.5 High resolution isotopic mapping

A root was sectioned from a switchgrass plant exposed to a $^{13}CO_2$ label. The source plant was grown in a rhizobox partially filled with sandy loam Alfisol soil (43% sand, 40% silt, 17% clay; Robertson et al. 1997) acquired from the W. K. Kellogg Biological Station (KBS; Hickory Corners, Michigan USA) that was mixed with an organic phosphorous treatment to promote growth. Rhizoboxes (12.5 cm × 19 cm x 1.9 cm) were constructed with sheets of high-density polyethylene (Denis et al. 2019) designed to facilitate root access (Huck and Taylor 1982). Seeds were germinated hydroponically and then transplanted into the rhizoboxes (at roughly 5 days old) and grown in a Conviron GR48 walk-in growth chamber for 12 weeks. For application of the $^{13}CO_2$ tracer, rhizoboxes were placed in a sealed chamber (51 x 64 x 90 cm) containing a single septum port and placed into the growth chamber. An initial 300 mL (at STP) of $^{13}CO_2$ (99 atom % $^{13}CO_2$, Sigma Aldrich, St. Louis, Missouri, USA) was injected into the chamber followed by a secondary injection (150 mL) after 24 hours to compensate for CO_2 loss through photosynthesis. After 48 hours, rhizoboxes were removed from the chamber. This labeling duration (48 hours) was shown in previous experiments to provide significant ^{13}C accumulation in portions of the resulting plant tissues and in the more recent (≤ 48 hours old) root exudates. The juxtaposition of carbon derived from recent photosynthate (with an elevated $\delta^{13}C$) with pre-existing carbon (with natural abundance $\delta^{13}C$, from before the initiation of $^{13}CO_2$ exposure) offered spatial $\delta^{13}C$ gradients within the sample which were ideal for demonstrating the LA-CAS capability. The above-soil plant biomass was cut at the base of the stem, placed in paper autoclave bags, dried at room temperature for 10 days and then transferred to an oven (70 °C) to ensure dryness. Rhizoboxes were stored in a freezer (-20 °C) until sample preparation for LA-CAS analysis.

The root cross section was positioned upright within a trench cut into a piece of plastic allowing for a top-down view. Pre-analysis photos were taken using a high magnification stereo microscope (Olympus SZH10) and integrated camera (Olympus Highlight 3000 reflected light source). Gridded X and Y coordinates were assigned to the 1x1 mm area of the root as µm units of distance from using a chosen point (X:Y, 0 µm:0 µm). The start and end coordinates for each continuous line ablation pass (25 µm spot size at 5 µm sec-1) were logged and used to assign coordinates to each individual $\delta^{13}C$ measurement. Line ablations were bracketed with sampling of fishing line to allow for calibration of root $\delta^{13}C$. A total of 60, line ablations were completed throughout the vascular tissue within the inner boundary of the cortex. Each calibrated $\delta^{13}C$ measurement (Z) and their associated coordinates (X,Y) were plotted as a heat map using Origin 2021b graphing software (see section 3.4 and **Fig. 7**).

We then expanded this approach by mapping a larger area (3.3x2.4 mm) of a puck with ^{13}C labeled soil and roots of varying thickness. As with the previous tests, we use fishing line for calibration. Procedure follows the same as described in the previous paragraph with results presented in **Fig. 8**.

2.4 *Statistical handling of results*

As this is a novel application of a relatively new instrument, it is challenging to fully consider the results of this study in terms of conventional statistical analysis. However, we would not expect a homogenous distribution of carbon isotopes in biological material with or without isotopic pulse labeling which makes comparison of replicate sample analyses infeasible. Thus, it is improbable that application of conventional statistical tests would appropriately characterize the significance of the data. Although we partially represent and interpret the results qualitatively, the observed degree of replication is sufficient evidence to support further deployment of LA-CAS and improvements to data validation.

3. Results

3.1 Quantification of analyte flow rate through LA-CAS

The first appearance of analyte in the CAS occurred 6.2 ± 0.3 seconds (mean ± standard deviation; 7 analytical replicates) after initial contact of the laser ablation beam with the Lexan surface; indicating a 6.2 second sample lag time linked to movement of particulates and resulting CO_2 through the system. A plateau in ^{13}C concentration (ppm) occurred at a mean value of 85.9 ± 1.9 ppm beginning at 9.9 ± 0.6 seconds (**Fig. 2**). The last sample reaching the detector occurred 4.1 ± 0.4 seconds after ablation ceased. A return to baseline (attributed to the constant contribution of low levels of CO_2 in the He-carrier gas), pre-ablation ^{13}C concentration values was achieved 9.8 ± 0.8 seconds following the end of ablation.

3.2 Continuous line ablation over isotopically distinct surfaces

When performing a continuous laser ablation scan, the first 788 μm of the path (associated with just the Lexan) had a mean calibrated $\delta^{13}C$ value of 14.2 ± 3.5 ‰ (**Fig. 3**). There was a delay of 6.6 seconds from the first contact of the beam with the Lexan-stem boundaries to when the ablated sample reached the detector. The measured $\delta^{13}C$ for stem material between 1184-2011 μm (from the starting position of the scan) had a range of 118.6-216.2‰. Analysis of the subsequent 1675 μm (from 2011 to 3686 μm) of stem featured a notable increase in $\delta^{13}C$ with peak values of 415-512‰. Notably, peaks in $\delta^{13}C$ seen in **Fig. 3** occur between the grooves of the stem with the number of peaks matching the number of ridges (11). The measured $\delta^{13}C$ near both plastic-stem boundaries was noticeably lower relative to the analyte originating from the stem interior. A second pass in the reverse direction was made parallel to the ablation path in **Fig. 3** and these features, including the trend in stem $\delta^{13}C$, were replicated.

Calibrated $\delta^{13}C$ of analyte sourced from spot ablation with trapping was compared to data acquired from continuous flow line ablation. The trend in $\delta^{13}C$ from soil to fishing line was consistent with $\delta^{13}C$ measured through spot ablation (**Fig. 4**). The average $\delta^{13}C$ of soil during continuous flow measurements in proximity to the first (-25.0‰) and third (-28.7‰) spot ablations were within the error of the corresponding spot ablation (-28.2 ± 3.5‰ and -29.7 ± 4.2‰). Similarly, peaks in $\delta^{13}C$ for analyzed soil during continuous flow closely corresponded to the values for spot ablations 1 through 6, but appeared to differ from spot ablations 7-10, possibly indicating more heterogenous material. Although the line ablation data also had an observed increase in $\delta^{13}C$ as the beam approached the root, the results contrasted with the spot ablation data. These differences are discussed further in section 4.1. In subsequent data collections over the soil-rhizosphere-root continuum we adjusted the scan rate and spot size when approaching thin roots. This enabled LA-CAS to better capture (and at improved spatial resolution) the increase in $\delta^{13}C$ as the scan approaches the root in addition to the increasing $\delta^{13}C$ from the outer to inner sections of the root (**Fig. 5**).

3.3 Continuous flow segmented line ablation in forward and reverse directions

A near instantaneous response was observed in $\delta^{13}C$ associated with the material as the scan proceeded in both directions. The $\delta^{13}C$ profile for both directions are similar in terms of trends in $\delta^{13}C$ as well as average values for specific associated locations (**Fig. 6**). Measurements taken on the internal section of the root had a mean $\delta^{13}C$ value of -18.5 ± 1.3‰, comparable with the same location during the second pass (-19.9 ± 1.2‰). Soil $\delta^{13}C$ values were more variable ranging from -30 to -40‰. While the trends between the forward and reverse transects corroborate each other, it is unclear why some measured $\delta^{13}C$ values for soil reach such ^{13}C depleted values. Future efforts should focus on developing suitable matrix-matched stable isotope standards (presumably of soil or similar material) to address this potential issue.

3.4 High spatial resolution isotope mapping of plant biomass

The 60 line scans (10 µm spot size at 5 µm sec^{-1}) represent a total of 2954 individual CAS measurements that, along with data processing and assigning gridded locations, was completed in ~7 total hours of instrument time. Over the entire root profile, calibrated $\delta^{13}C$ values range from -20-260‰. The most ^{13}C depleted (-20 to 15‰) regions occurred where the ablation passes were near and intersected with the cortex (**Fig. 7**). The $\delta^{13}C$ measurements taken on the pith (central section of root) were also low (30 to 40‰) relative to the surrounding area. The highest $\delta^{13}C$ values (200 to 260‰) generally occurred between each respective xylem with a few exceptions. A ^{13}C-hotspot (in the inter-xylem space) such as these was absent in the lower left section of the root (**Fig. 7**; X,Y: 300,700 µm). Ablation scans directly over and in proximity to the xylem featured the most variable $\delta^{13}C$ values ranging from 100 to 140‰. A similar scan was performed over a sample section containing a large and small root with the surrounding rhizosphere and soil (**Fig. 8**). Damage caused by the laser ablation process ejected a section of a targeted root. The data do, however, enable mapping of the $\delta^{13}C$ on the sample surface and demonstrate regions of higher ^{13}C in the smaller versus larger root captured in the image.

4. Discussion

4.1 Assessment of continuous flow LA-CAS

The time related data detailing the flow rates of analyte from ablation to detector indicate a very consistent and repeatable process. The lag between the start of laser ablation and first detection of sample (6.2 ± 0.3 seconds) with CAS varied only slightly across multiple replicate analyses. Measured $\delta^{13}C$ stabilized around the mean value for the plastic test material at ~3.5 seconds after first detection (**Fig. 2**), which suggests the approach can capture changes in $\delta^{13}C$ that occur over short spatial distances. Additionally, the pronounced similarity between the time required to reach the mean $\delta^{13}C$ value of the material (9.9 ± 0.6 seconds following initial ablation of the material) and for a sample to be completely evacuated (9.8 ± 0.8 seconds after ceasing ablation of the material) suggested limited mixing throughout each individual scan, and that pulses of material propagate through the system as a distinct front. It should be noted that (to the best of our knowledge and experience) the Lexan material is isotopically homogenous and has much higher total carbon abundance versus soil or rhizosphere samples.

The rates of flow through the CAS system did not change when mounting the dried switchgrass stem on the plastic sample holder. Analysis of $\delta^{13}C$ for the ablation transect over plastic and switchgrass stem effectively captured the boundary between the isotopically distinct surfaces (**Fig. 3**). Scans were completed for 25 µm spot sizes at speeds of 5 and 10 µm sec^{-1} with near complete overlap between each respective $\delta^{13}C$ profile. The primary distinction is that a speed of 5 µm sec^{-1} provides a higher density of data points at the cost of analysis time (2x as long). The slight variation in the measured $\delta^{13}C$ between the two scans likely reflects the spatial variability in the plant stem where the periodic increase and decrease in the $\delta^{13}C$ trace most likely reflects the vasculature (and different $\delta^{13}C$) in the stem sample itself. However, an alternative explanation could be that the curvature of the sample led to slight defocusing of the laser and created sampling artifacts consistent with the contrasting values of $\delta^{13}C$ between the left (1184-2011 µm) and right sides of the stem. While this appears unlikely (as one would expect similar curvature on each side of the stem), more thorough examination of the impact of sample surface topography on measured $\delta^{13}C$ values should be explored in the future to gauge its potential impact on both LA-CAS and LA-IRMS approaches.

The ^{13}C-enriched ridges of the stem (**Fig. 3**) are associated with products of photosynthesized $^{13}CO_2$ captured in the stem during the freezing of the plant-rhizobox. Within monocot plants, such as switchgrass (Mann et al. 2012), photosynthates are transported through along vascular bundles scattered along the edge of the stem (Chase 2004). The phloem within these tissues operate as a hydrostatic driven transport system that allows the flow of photosynthates (carbohydrates and amino acids) from the leaves and upper region of the plant down to the roots system in the subsurface (Baslam et al. 2020; Lambers et al. 2009). Presumably these observed morphological ridges correspond with these vascular bundles that have become more pronounced following desiccation of the surrounding tissue. Therefore, it is plausible the observed $\delta^{13}C$ peaks result from the continuous ablation path alternating between ^{13}C-labelled photosynthates concentrated in vascular bundles (ridges) and cortex/epidermis tissues that feature a contrasting low $\delta^{13}C$. This provides an example of the how the spatially explicit analysis afforded by continuous flow LA-CAS can capture isotopically distinct features within a single continuous line scan ablation.

Similar to the Lexan-root analysis (**Fig. 3**), CAS effectively captured changes in $\delta^{13}C$ as the line scan transitioned across soil, fishing line, and root boundaries (**Fig. 4**). Mean $\delta^{13}C$ values for spot ablations near the line scan paths generally agree with soil and fishing line values prior to the root. However, a notable deviation occurs between spot ablations 8 and 9 near the root (**Fig. 4**), with the spot ablation $\delta^{13}C$ value substantially lower than the $\delta^{13}C$ from continuous flow. The reason for the discrepancy could be due to the size of the root and scan rate which did not allow sufficient time to capture the true $\delta^{13}C$. As demonstrated (**Fig. 5**), if a sample has thin or brittle roots, the best laser operating parameters are 10 µm spot size moving at 5 µm sec^{-1}. This would indicate alternating between different spot sizes and scan rates for soil and roots may be preferred and possible if the user performs a higher density of scans. Such an approach with LA-CAS would better capture high spatial resolution variation in $\delta^{13}C$ as the scan approaches the inter-root material. However, this may not be necessary for samples with larger root structures.

4.2 Isotope mapping

A previous limitation to $\delta^{13}C$ measurements by laser ablation sampling was the need for cryotrapping CO_2 generated from the sample (Grieve et al. 2006; Denis et al. 2019; Rodionov et al. 2019; Moran et al. 2022). This necessitated performing distinct measurements at individual, spatially resolved points along a sample which limited sample throughput (and resulting spatial density of data) due to the time required for cryogenic focusing of an analyte prior to isotopic measurement. In contrast to this limitation, the replication of $\delta^{13}C$ values in forward and reverse paths during our continuous flow approach for analyzing the segmented line scan (**Fig. 6**) suggests that the improved sensitivity of CAS permits scans to be run continuously with LA-CAS without sacrificing spatial resolution. In this case, depth of focus did not change significantly between first scan and return scan, allowing for self-consistent $\delta^{13}C$ results. When applying this approach and performing a high-density analysis of a 1x1 mm root cross-section it is possible to produce a highly spatially resolved isotope map of root features (**Fig. 7**). Unlike vascular tissues in the monocot stems that are scattered throughout, these features are organized in a ring (**Fig. 7**; microscope image) around the pith (Taiz and Zeiger 2002). Xylem vessels (**Fig. 7**) form a conduit that allow transport of water and nutrients from the roots to the above ground biomass of the plant (Baslam et al. 2020). The ^{13}C-enriched areas of this root occur between the visible xylem structures in a location consistent with the presence of phloem. The observed increase in measured δ^{13}C in these areas is consistent with the transport of ^{13}C-labeled photosynthates from the leaves down through the roots as previously demonstrated by various short-term ^{11}C-tracer studies which likewise traced the transport of labelled assimilates to the phloem of different trees (De Schepper et al. 2013; McQueen et al. 2005).

The success of LA-CAS in facilitating the tracing of the distribution of these photosynthates within a root suggests the method could be applied to larger sampling areas of the rhizosphere. Line scans moving over an area of soil intersected by a length of root revealed higher δ^{13}C values for measurements taken in proximity to the root. One of the challenges of this method is weakening of root integrity with each additional continuous line scan over the surface due to the impact of laser ablation sampling. This is increasingly an issue when the root is thinner (younger) and/or brittle. In this example the root broke in a few instances, preventing the measurement of δ^{13}C for root in that location. However, sufficient successful scans were made to characterize the sampling area in terms of δ^{13}C. The highest measured δ^{13}C was found to be directly on the root surface while soil analyzed within 50-100 µm of the root had higher 13C enrichment than more distal soil. In contrast, measured δ^{13}C for larger root material within the sampling area (**Fig. 8**; left side of image) was lower relative to the thinner root which was potentially growing (i.e., accreting ^{13}C labeled photosynthate at the time of sampling). The ^{13}C-enriched areas identify the spatial distribution and location of root exudates within the sample. The difference in measured δ^{13}C between the two roots could be related to the relationship between root exudation and root growth stage. Relative to older roots, younger root zones have a higher capacity for nutrient uptake (Fang et al. 2007) and could thus deliver more exudates (Marschner et al. 2011), particularly within the time period considered between labelling-sampling (Denis et al. 2019). Interestingly there are a few instances where a concentrated area of soil away from the root had anomalously high δ^{13}C (17-24‰) when compared to the typically ^{13}C-depleted soil. Similar occurrences were found in switchgrass rhizosphere samples by Denis et al. (2019) who attributed the hotspots to higher carbon delivery associated within increased microbial activity in these areas (Gutiérrez Castorena et al. 2016; Kravchenko et al. 2017).

4.3 LA-CAS analytical niche, cautions, and future directions

Laser ablation sampling coupled to real-time analysis of the resulting particulate plume is a well-established technique when coupled with inductively coupled mass spectrometry (ICP-MS) for elemental and stable isotope analysis within a wide variety of geologic and biologic sample types (Jenner and Arevalo 2016; Becker et al., 2014). However, LA-ICP-MS is unable to perform $\delta^{13}C$ analysis due to limitations associated with the plasma source used on ICP instruments. Spatially resolved $\delta^{13}C$ measurements at the 10s µm scale have been developed using LA sampling of a sample surface coupled to isotope evaluation using IRMS. Yet, existing LA-IRMS methods employ cryofocusing to help overcome sample size requirements for IRMS analysis and, as a result of the time-dependence of cryotrapping, sample throughput cannot come close to matching those of LA-ICP-MS. The LA-CAS approach we present here leverages the sensitivity of CAS to circumvent the cryotrapping requirement inherent to LA-IRMS and enables isotopic measurement in near real time with sample ablation. This "continuous flow" method drastically improves sample throughput compared to LA-IRMS which enables increased data collection over a sample surface where the resulting increase in data density can improve the ability for mapping the $\delta^{13}C$ of a sample surface. As with any LA-based approach, care needs to be taken to ensure the accuracy of the resulting data. For example, if not properly performed, LA sampling can be biased towards components within a sample having higher ablation efficiency when heterogeneously dispersed over a sample's surface. In other cases, the agnostic nature of LA can introduce a background effect to a sample. For example, ablation of a carbonate-rich soil could produce an undesirable C background and limit the sensitivity of LA-CAS to tracking organics (e.g., root exudates) in the sample. For some cases, the ablation may need to be controlled to avoid unwanted drilling into the sample surface which may reveal underlying sample complexity which was neither visible from the surface nor intended to be part of a surface map. Further, matrix effects must be considered where, for example, ablation efficiency can be impacted by the specific physical properties of the sample. Ideally, matrix matching of sample and standard materials would be used to help control this artifact, but the broad diversity of soil matrix types can complicate these efforts. Future efforts in spatial resolved $\delta^{13}C$ measurements (both LA-CAS and LA-IRMS) need to address the paucity of matrix-matched standards available to the field. LA is also (by its very nature) a destructive technique where material is removed from a sample. The high impacting energy of LA can damage a sample as observed in some of the described measurements above (e.g., within **Fig. 8**). In these cases, one needs to critically evaluate whether the benefits of improved sampling density (by the "continuous flow" method described here) outweigh the increased amount of damage to a sample surface and resulting loss of material. Finally, effective analysis requires balancing the amount of CO_2 produced from LA with the quantity that can be measured using the appropriate detector (e.g., CAS or IRMS). Spatial variability within samples can create large swings in the amount of CO_2 produced per ablation where the linearity of the instrument response needs to be considered in assessing measurement accuracy. While future work needs to address the above challenges, the demonstrations presented here show the ability of LA-CAS to contribute to spatially resolved $\delta^{13}C$ measurements in plant and soil systems and highlight the benefits of LA-CAS for mapping $\delta^{13}C$ distribution in these systems.

5. Conclusions

This work demonstrates the potential of continuous flow LA-CAS for tracing the distribution of ^{13}C-labeled nutrients through the plant, root, rhizosphere, and soil. The high sampling rate and short instrument/data processing time allow for high spatial resolution mapping of large sampling areas in a few hours. Such advantages relative to other analytical techniques may prove LA-CAS to be an ideal alternative for tracking spatial variability in $\delta^{13}C$ at μm resolution over >4 mm^2 areas.

6. Acknowledgements

System development and testing of the approach was funded by the US Department of Energy (DOE) Office of Biological and Environmental Research by both the Small Business Technology Transfer program, Grant DE-SC0018488 (PI: J. Kriesel) and the Early Career Research Award program (PI: J. Moran). A portion of this research was performed on a project award (51793) from the Environmental Molecular Sciences Laboratory, a DOE Office of Science User Facility sponsored by the Biological and Environmental Research program under Contract No. DE-AC05-76RL01830.

Figures

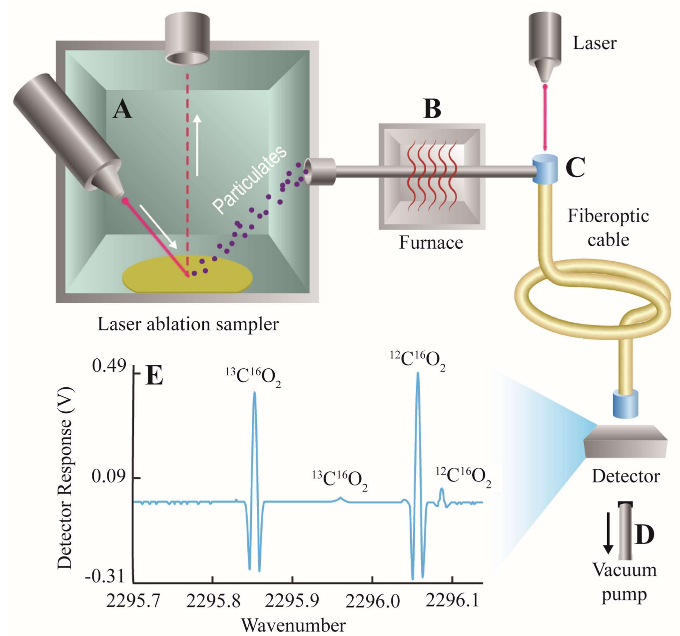

Figure 1: Schematic of LA-CAS configuration. A) ablation of sample within laser ablation instrument, B) particulates combusted, C) entry of analyte into CAS fiber, D) sample removal via vacuum, and E) measurement taken at detector.

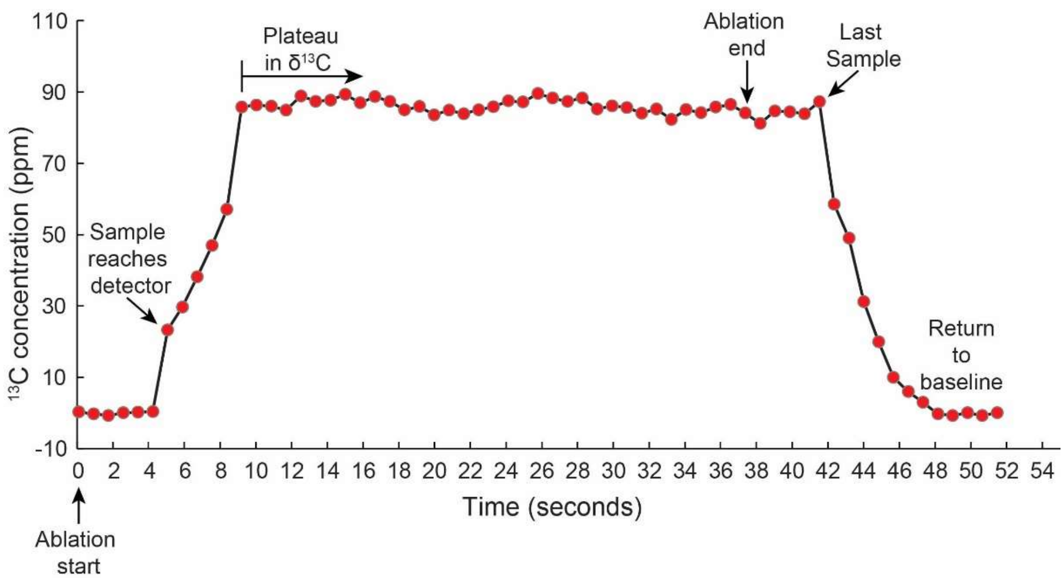

Figure 2: Representative chromatogram of the timing of events during continuous flow measurements completed with LA-CAS. T_1) beginning of ablation, T_2) sample arrives at detector, T_3) plateau in signal, T_4) end of ablation, T_5) last ablated sample at detector and T_6) return to baseline.

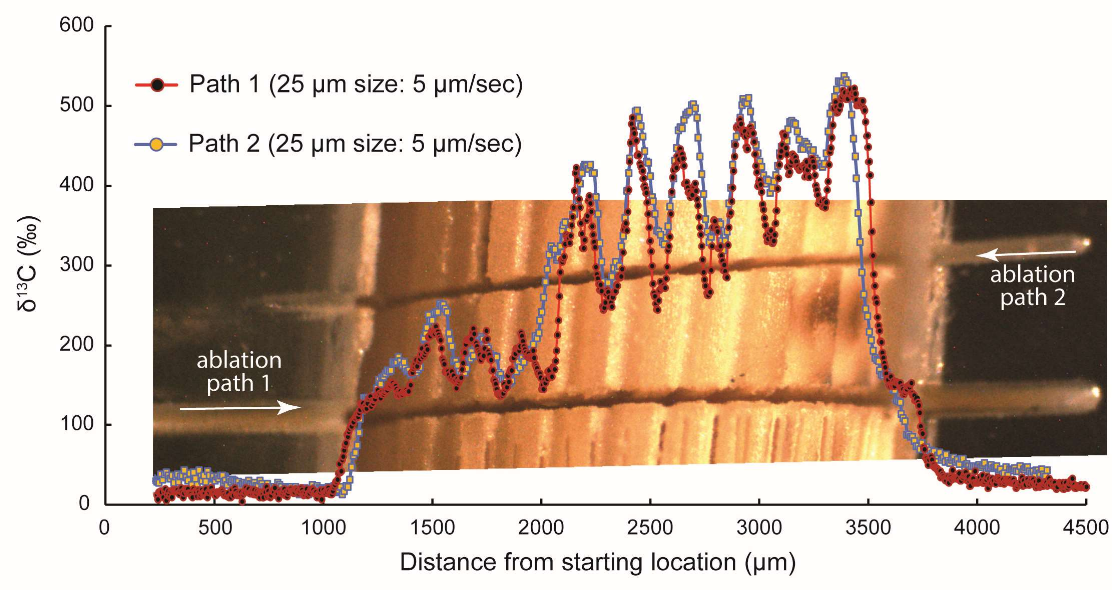

Figure 3: Continuous scan ablation over isotopically distinct materials demonstrates the ability of LA-CAS to capture spatial variation in $\delta^{13}C$.

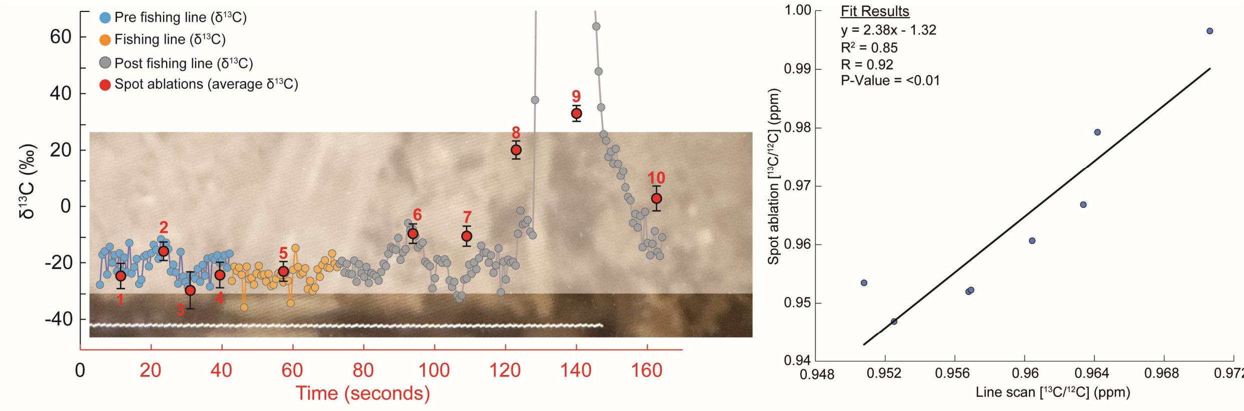

Figure 4: $\delta^{13}C$ of material from spot ablations is comparable to measured $\delta^{13}C$ from corresponding material ablated with continuous line scans. The scan passes over soil, fishing line (~40-70 seconds; used as an isotope calibration standard, soil, and root (~125-155 seconds) portions of the sample. Spot ablation points are numbered 1-10 (red) from left to right. Direct comparison of the spot scans with representative portion of the line scan demonstrate reasonable correlation (R2=0.85) although it should be noted that the spot ablations were performed near (but not on top of) the line scan and spatial variability in the sample is expected to preclude identical measured values between the two data sets.

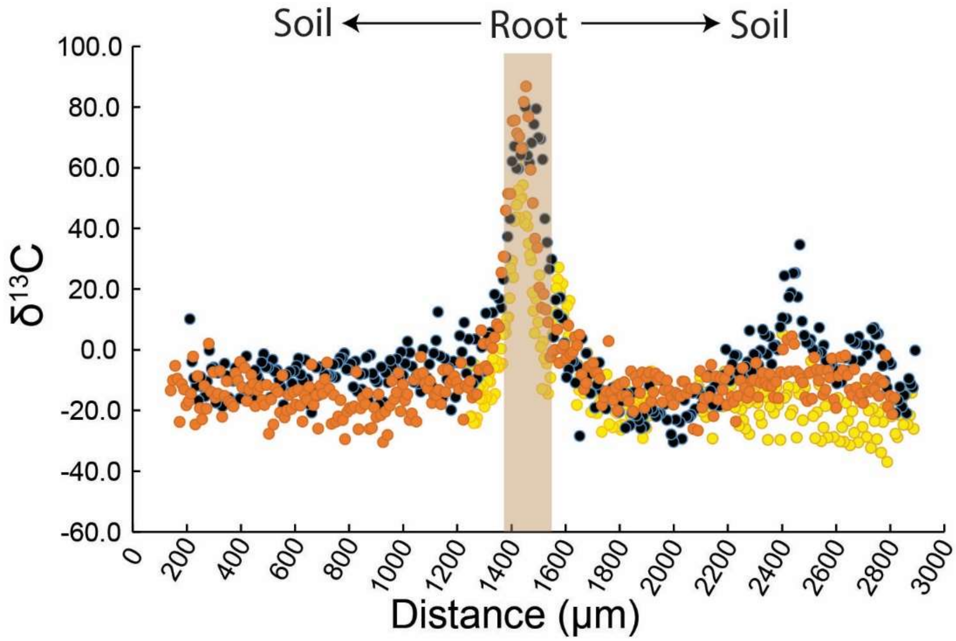

Figure 5: Repeated scans over root with different spot size and scan rates for root (10 µm spot size / 5 µm sec^{-1}) and soil (25 µm spot size / 10 µm sec^{-1}). The colors in the points depict data collected on three transects made in nearby locations of the sample.

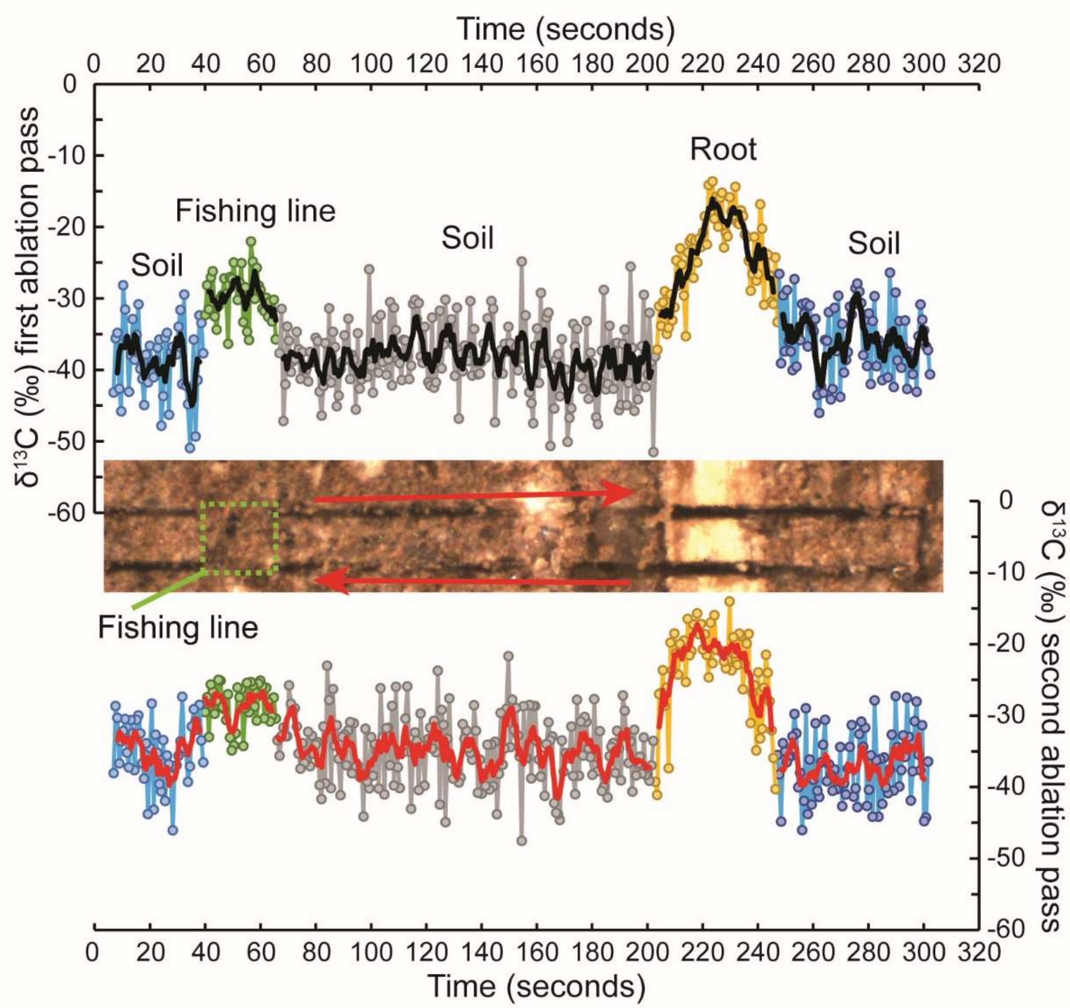

Figure 6: Reversing path of laser scan and varying beam size yields the same measured $\delta^{13}C$ values. Smallest usable beam size depends on material being ablated. For ^{13}C labeled material, best results were 10 µm spot diameter for stem and root at scan rates of 5 µm/sec and 25 µm/sec respectively. Solid black and red lines represent a 2.7 sec moving average over individual data.

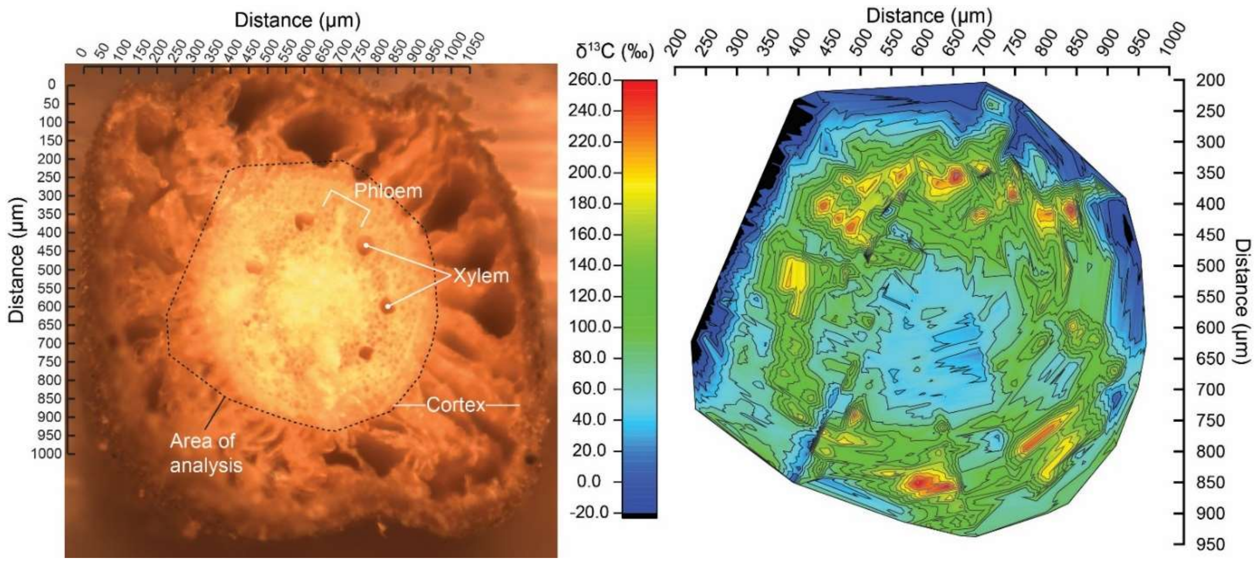

Figure 7: Contour map of $\delta^{13}C$ values across the top view of a ^{13}C-labeled switchgrass root. Xylem location indicated by white outline. Continuous scans made with a 10 µm beam size and moving at 5 µm sec^{-1}.

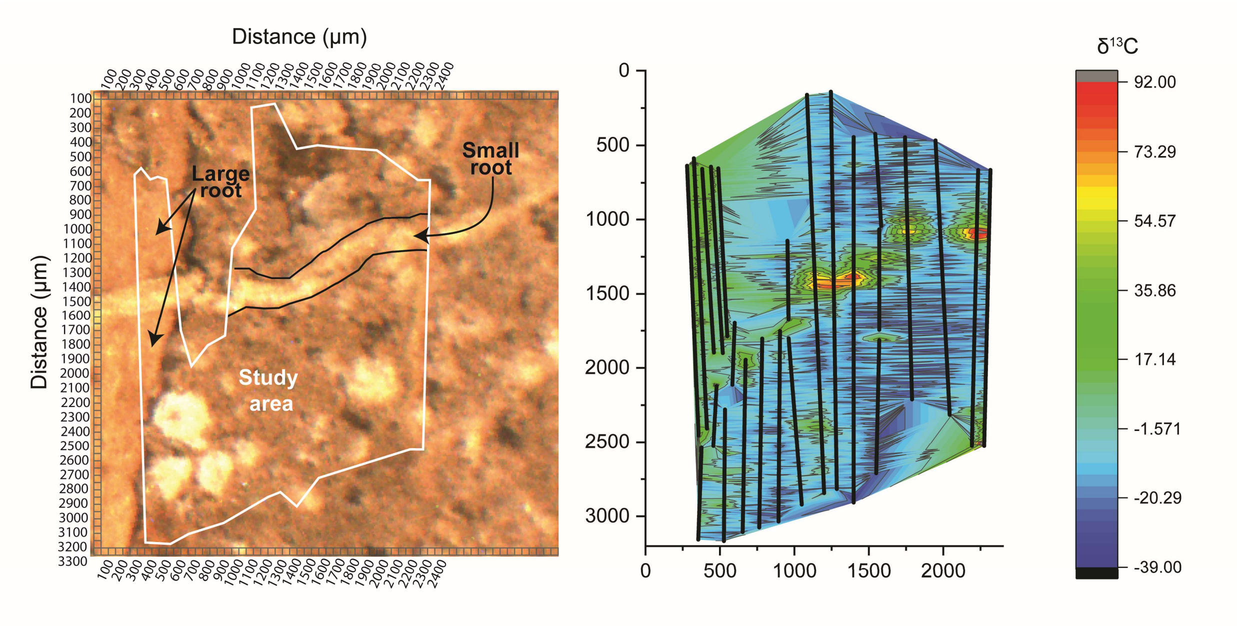

Figure 8: Contour map of δ^{13}C values of ^{13}C-labeled switchgrass root and rhizosphere soil. Light microscope image (left) with area of analysis indicated (white border).

References

Bais HP, Weir TL, Perry LG, Gilroy S, Vivanco JM (2006) The Role of Root Exudates in Rhizosphere Interactions with Plants and Other Organisms. Annual Review of Plant Biology 57: 233-266. doi: 10.1146/annurev.arplant.57.032905.105159.

Baslam M, Mitsui T, Sueyoshi K, Ohyama T (2020) Recent Advances in Carbon and Nitrogen Metabolism in C3 Plants. International Journal of Molecular Sciences 22. doi: 10.3390/ijms22010318.

Becker JS, Matusch A, Wu B (2014) Bioimaging mass spectrometry of trace elements – recent advance and applications of LA-ICP-MS: A review. Analytica Chimica Acta 835: 1-18. doi:10.1016/j.aca.2014.04.048

Bird JA, Herman DJ, Firestone MK (2011) Rhizosphere priming of soil organic matter by bacterial groups in a grassland soil. Soil Biology and Biochemistry 43: 718-725. doi: 10.1016/j.soilbio.2010.08.010.

Bruneau PMC, Ostle N, Davidson DA, Grieve IC, Fallick AE (2002) Determination of rhizosphere ^{13}C pulse signals in soil thin sections by laser ablation isotope ratio mass spectrometry. Rapid Communications in Mass Spectrometry 16: 2190-2194. doi: 10.1002/rcm.740.

Chase MW (2004) Monocot relationships: an overview. American Journal of Botany 91: 1645-1655. doi: 10.3732/ajb.91.10.1645.

Cleary DM, Linley T, Kriesel J, Fahrland A, Kelly JF, Moran JJ (2021) Capillary absorption spectroscopy for high temporal resolution measurements of stable carbon isotopes in soil and plant-based systems. Plant Physiology and Biochemistry 169: 1-8. doi: 10.1016/j.plaphy.2021.10.025.

Clode PL, Kilburn MR, Jones DL, Stockdale EA, Cliff JB, Herrmann AM, Murphy DV (2009) In Situ Mapping of Nutrient Uptake in the Rhizosphere Using Nanoscale Secondary Ion Mass Spectrometry. Plant Physiology 151: 1751-1757. doi: 10.1104/pp.109.141499.

De Schepper V, Bühler J, Thorpe M, Roeb G, Huber G, van Dusschoten D, Jahnke S, Steppe K (2013) 11C-PET imaging reveals transport dynamics and sectorial plasticity of oak phloem after girdling. Frontiers in Plant Science 4. doi: 10.3389/fpls.2013.00200.

de Vrieze J (2015) The Littlest Farmhands. Science 349: 680-683.

Denis EH, Ilhardt PD, Tucker AE, Huggett NL, Rosnow JJ, Moran JJ (2019) Spatially tracking carbon through the root–rhizosphere–soil system using laser ablation-IRMS. Journal of Plant Nutrition and Soil Science 182: 401-410. doi: 10.1002/jpln.201800301.

Fang YY, Babourina O, Rengel Z, Yang XE, Pu PM (2007) Spatial distribution of ammonium and nitrate fluxes along roots of wetland plants. Plant Science 173: 240-246. doi: 10.1016/j.plantsci.2007.05.006.

Grieve IC, Davidson DA, Ostle NJ, Bruneau PMC, Fallick AE (2006) Spatial heterogeneity in the relocation of added ^{13}C within the structure of an upland grassland soil. Soil Biology and Biochemistry 38: 229-234. doi: 10.1016/j.soilbio.2005.04.035.

Gutiérrez Castorena EV, Gutiérrez-Castorena MdC, González Vargas T, Cajuste Bontemps L, Delgadillo Martínez J, Suástegui Méndez E, Ortiz Solorio CA (2016) Micromapping of microbial hotspots and biofilms from different crops using digital image mosaics of soil thin sections. Geoderma 279: 11-21. doi: 10.1016/j.geoderma.2016.05.017.

Hinsinger P, Bengough AG, Vetterlein D, Young IM (2009) Rhizosphere: biophysics, biogeochemistry and ecological relevance. Plant and Soil 321: 117-152. doi: 10.1007/s11104-008-9885-9.

Hinsinger P, Gobran GR, Gregory PJ, Wenzel WW (2005) Rhizosphere geometry and heterogeneity arising from root-mediated physical and chemical processes. New Phytologist 168: 293-303. doi: 10.1111/j.1469-8137.2005.01512.x.

Hodge A (2004) The plastic plant: root responses to heterogeneous supplies of nutrients. New Phytologist 162: 9-24. doi: 10.1111/j.1469-8137.2004.01015.x.

Holz M, Zarebanadkouki M, Kuzyakov Y, Pausch J, Carminati A (2018) Root hairs increase rhizosphere extension and carbon input to soil. Annals of Botany 121: 61-69. doi: 10.1093/aob/mcx127.

Huck MG, Taylor HM (1982) The Rhizotron as a Tool for Root Research. Advances in Agronomy Volume 35.

Jenner FE, Arevalo R.D. Jr. (2016) Major and trace element analysis of natural and experimental igneous systems using LA-ICP-MS. Elements 12: 311-316. doi: 10.2113/gselements.12.5.311.

Kelly JF, Sams RL, Blake TA, Newburn M, Moran J, Alexander ML, Kreuzer H (2012) A capillary absorption spectrometer for stable carbon isotope ratio ($^{13}C/^{12}C$) analysis in very small samples. Review of Scientific Instruments 83. doi: 10.1063/1.3680593.

Kravchenko AN, Toosi ER, Guber AK, Ostrom NE, Yu J, Azeem K, Rivers ML, Robertson GP (2017) Hotspots of soil N_2O emission enhanced through water absorption by plant residue. Nature Geoscience 10: 496-500. doi: 10.1038/ngeo2963.

Kriesel JM, Makarem CN, Fahrland A, Moran JJ, Linley T, Kelly JF, Razeghi M, Lewis JS, Khodaparast GA, Khalili P (2020) Hollow fiber mid-IR spectrometer with UV laser ablation sampling for fine spatial resolution of isotope ratios in solids. Quantum Sensing and Nano Electronics and Photonics XVII.

Kuzyakov Y, Blagodatskaya E (2015) Microbial hotspots and hot moments in soil: Concept & review. Soil Biology and Biochemistry 83: 184-199. doi: 10.1016/j.soilbio.2015.01.025.

Kuzyakov Y, Domanski G (2000) Carbon input by plants into the soil. Review. Journal of Plant Nutrition and Soil Science 163: 421-431. doi: 10.1002/1522-2624(200008)163:4<421::Aid-jpln421>3.0.Co;2-r.

Lambers H, Mougel C, Jaillard B, Hinsinger P (2009) Plant-microbe-soil interactions in the rhizosphere: an evolutionary perspective. Plant and Soil 321: 83-115. doi: 10.1007/s11104-009-0042-x.

Li J, Li R, Zhao B, Guo H, Zhang S, Cheng J, Wu X (2018) Quantitative measurement of carbon isotopic composition in CO_2 gas reservoir by Micro-Laser Raman spectroscopy. Spectrochimica Acta Part A: Molecular and Biomolecular Spectroscopy 195: 191-198. doi: 10.1016/j.saa.2018.01.082.

Mann DGJ, LaFayette PR, Abercrombie LL, King ZR, Mazarei M, Halter MC, Poovaiah CR, Baxter H, Shen H, Dixon RA, Parrott WA, Neal Stewart Jr C (2012) Gateway-compatible vectors for high-throughput gene functional analysis in switchgrass (Panicum virgatum L.) and other monocot species. Plant Biotechnology Journal 10: 226-236. doi: 10.1111/j.1467-7652.2011.00658.x.

Marschner P, Crowley D, Rengel Z (2011) Rhizosphere interactions between microorganisms and plants govern iron and phosphorus acquisition along the root axis – model and research methods. Soil Biology and Biochemistry 43: 883-894. doi: 10.1016/j.soilbio.2011.01.005.

McQueen JC, Minchin PEH, Thorpe MR, Silvester WB (2005) Short-term storage of carbohydrate in stem tissue of apple (Malus domestica), a woody perennial: evidence for involvement of the apoplast. Functional Plant Biology 32. doi: 10.1071/fp05082.

Moran, JJ, Newburn MK, Alexander ML, Sams RL, Kelly JF, Kreuzer HW (2011) Laser ablation isotope ratio mass spectrometry for enhanced sensitivity and spatial resolution in stable isotope analysis. Rapid Communications in Mass Spectrometry 25, 1282-1290.

Moran J, McGrath C (2021) Comparison of methods for mapping rhizosphere processes in the context of their surrounding root and soil environments. BioTechniques 71: 604-614. doi: 10.2144/btn-2021-0021.

Moran, J, Linley, TJ, Makarem, CN, Kelly, JF, Freeburg, EDW, Cleary, DM, Alexander, ML, Kriesel, JM (2022) Spectroscopy-based isotopic ($\delta^{13}C$) analysis for high spatial resolution of carbon exchange in the rhizosphere. Rhizosphere 23: 100564. doi: 10.1016/j.rhisph.2022.100564.

Pausch J, Kuzyakov Y (2018) Carbon input by roots into the soil: Quantification of rhizodeposition from root to ecosystem scale. Global Change Biology 24: 1-12. doi: 10.1111/gcb.13850.

Robertson GP, Klingensmith KM, Klug MJ, Paul EA, Crum JR, Ellis BG (1997) Soil Resources, Microbial Activity, and Primary Production across an Agricultural Ecosystem. Ecological Applications 7: 158-170. doi: 10.1890/1051-0761(1997)007[0158:Srmaap]2.0.Co;2.

Rodionov A, Lehndorff, E, Stremtan, CC, Brand, WA, Königshoven, H-P, Amelung, W (2019) Spatial microanalysis of natural $^{13}C/^{12}C$ abundance in environmental samples using laser ablation-isotope ratio mass spectrometry. Analytical Chemistry 91: 6225-6232. doi: 10.1021/acs.analchem.9b00892.

Taiz L, Zeiger E (2002) Plant physiology. Sinauer associates.